TransAneu-Net: A Hybrid Radiomics and Contrastive Deep Learning Framework for Automated Brain Aneurysm Diagnosis

Zhadra Kozhamkulova[1]*, Shirin Amanzholova[2], Bella Tussupova[3],
Yelena Satimova[4], Mukhamedali Uzakbayev[5], Kenzhekhan Kaden[6], Dastan Kambarov[7]
UC Davis, California[1]
Kurmangazy Kazakh National Conservatory, Almaty, Kazakhstan[2]
Gumarbek Daukeyev Almaty University of Power Engineering and Telecommunications, Almaty, Kazakhstan[3, 4, 5, 6, 7]

***Abstract*—Accurate and early detection of intracranial aneurysms is critical for preventing life-threatening subarachnoid hemorrhage and improving clinical outcomes. This study proposes a hybrid diagnostic framework that integrates radiomics-based feature engineering with a transformer-driven deep learning architecture enhanced by teacher–student contrastive representation learning. The workflow incorporates region-of-interest segmentation, handcrafted radiomic feature extraction, multimodal representation fusion, and probabilistic aneurysm localization using high-resolution MR and MRA imaging. Comprehensive experiments conducted on benchmark neuroimaging datasets demonstrate that the proposed model achieves high classification accuracy, stable convergence, and robust generalization across diverse anatomical and imaging conditions. Qualitative evaluations further reveal that heatmap-based confidence overlays reliably identify aneurysmal regions and closely align with ground-truth annotations. The contrastive learning module strengthens spatial and frequency-domain feature alignment, enabling effective training under limited supervision and reducing performance degradation associated with data heterogeneity. While limitations remain regarding dataset breadth and segmentation dependencies, the results indicate that this hybrid radiomics–AI framework offers a promising pathway toward automated aneurysm screening and clinical decision support. The proposed system has the potential to enhance diagnostic precision, mitigate inter-observer variability, and contribute to earlier intervention in neurovascular care.**

Keywords*—Aneurysm; deep learning; radiomics; transformer networks; contrastive learning; MR imaging; MRA; medical image analysis; aneurysm detection; neurovascular diagnostics

I. Introduction

The timely and accurate diagnosis of intracranial aneurysms remains a critical challenge in contemporary neuroimaging and clinical decision support systems. Brain aneurysms pose a significant risk of subarachnoid hemorrhage, a condition associated with high mortality and long-term disability, which underscores the need for early detection strategies capable of identifying subtle vascular abnormalities before rupture occurs [1]. Conventional diagnostic modalities such as computed tomography angiography and magnetic resonance angiography provide detailed anatomical information, yet their interpretation often depends on expert assessment, introducing subjectivity and potential variability in diagnostic outcomes [2]. As a result, artificial intelligence approaches [50], particularly deep learning, have emerged as powerful tools for enhancing diagnostic precision through automated feature extraction and pattern recognition [3].

In recent years, radiomics has gained substantial attention as a complementary methodology for quantitative characterization of vascular morphology and tissue heterogeneity by transforming medical images into high-dimensional feature spaces [4]. When combined with deep learning, radiomics enables the integration of handcrafted descriptors with hierarchical neural features, yielding more discriminative representations for aneurysm analysis [5]. Transformer-based architectures, especially vision transformers, have demonstrated strong capabilities in modeling long-range dependencies and capturing subtle structural variations in neurovascular images, offering performance advantages over traditional convolutional models [6]. Furthermore, contrastive learning frameworks have shown promise in semi-supervised and weakly supervised scenarios by aligning spatial and frequency-domain representations, thus improving generalization when labeled datasets are limited [7].

Despite these advances, several challenges persist, including variability in imaging protocols, limited annotated datasets, and the need for robust cross-domain generalization in clinical environments [8]. Developing hybrid architectures that combine radiomic signatures, segmentation-driven region-of-interest extraction, and contrastive representation learning presents a promising direction for addressing these limitations [9]. This research aims to build upon these developments by proposing an integrated radiomics–deep learning framework for accurate and reliable diagnosis of intracranial aneurysms.

II. Related Works

A. Brain Aneurysm

A brain aneurysm is a localized pathological dilation of a cerebral artery resulting from weakening of the vessel wall layers, typically involving the tunica media and internal elastic lamina. As illustrated in Fig. 1, the aneurysm often forms as a saccular outpouching that protrudes from an arterial bifurcation or curve, where hemodynamic shear stress is elevated. These weakened segments can gradually expand due to pulsatile

*Corresponding author.

blood flow, eventually becoming prone to rupture. When rupture occurs, blood extravasates into the subarachnoid space, leading to subarachnoid hemorrhage, a medical emergency associated with high mortality and significant neurological deficits. The pathophysiology of aneurysm formation is multifactorial, involving genetic predisposition, endothelial dysfunction, chronic inflammation, and biomechanical stress, all of which contribute to progressive vessel wall degeneration.

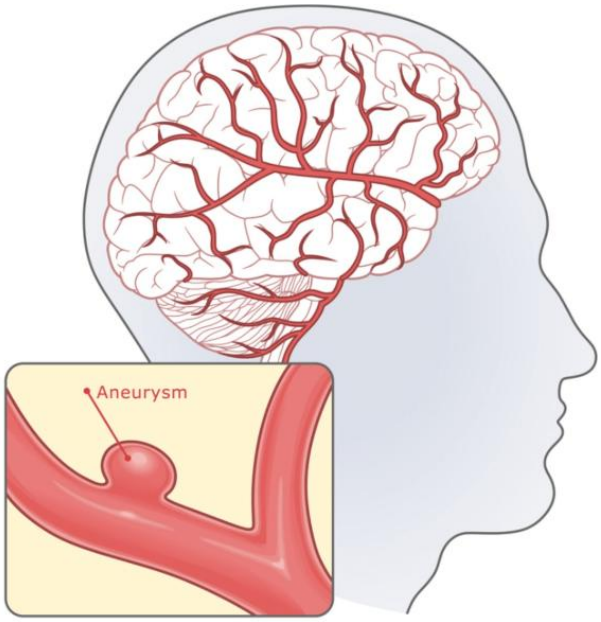

Fig. 1. Illustration of a cerebral aneurysm as a localized arterial outpouching in the brain.

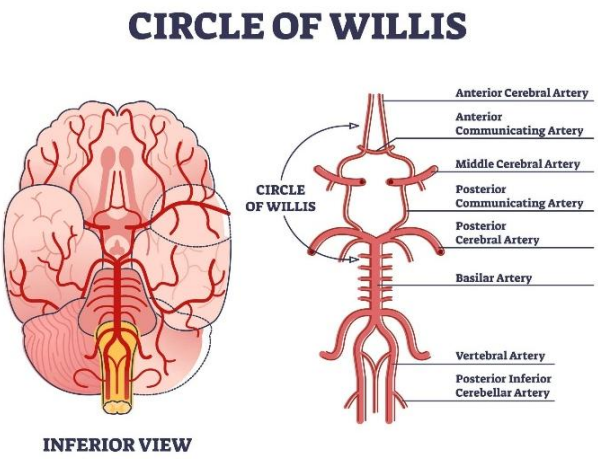

Fig. 2. Anatomical structure of the Circle of Willis, highlighting major cerebral arteries and common aneurysm sites.

The anatomical distribution of brain aneurysms is closely related to the cerebrovascular architecture, particularly the Circle of Willis, as shown in Fig. 2. This arterial ring includes major bifurcation points of the anterior, middle, and posterior cerebral arteries, which are the most common sites for aneurysm development due to complex flow dynamics and turbulent pressure gradients. Aneurysms in these regions may remain asymptomatic until enlargement or rupture occurs, although some may produce symptoms through mass effect or compression of adjacent cranial nerves. Understanding the vascular topology of the Circle of Willis is therefore essential for accurate diagnosis, risk stratification, and treatment planning, especially when integrating advanced imaging techniques and deep learning models that rely on precise localization of vascular anomalies.

B. Radiomics for Neurovascular Abnormality Detection

Radiomics has become a key methodological pillar for extracting quantitative biomarkers from neuroimaging data, enabling the transformation of complex aneurysmal morphology into structured high-dimensional feature sets [10]. Early studies demonstrated that handcrafted descriptors such as intensity histograms, texture matrices, and shape signatures provide discriminative cues for identifying abnormal vascular dilations in CTA and MRA images [11]. The reproducibility of radiomic features was further improved with standardized toolkits such as PyRadiomics, which introduced harmonized feature definitions and preprocessing protocols [12]. Such standardization has facilitated cross-institutional studies that reported enhanced sensitivity in aneurysm detection when radiomic features complement conventional clinical readings [13].

Subsequent investigations extended radiomics into multiscale characterizations, revealing that local heterogeneity and voxel-level variations correlate with aneurysm instability and rupture risk [14]. In particular, wavelet-based texture descriptors and Laplacian-derived edge patterns were shown to uncover microstructural abnormalities not readily visible to human observers [15]. Integration of radiomics with vessel segmentation algorithms, including automated region-of-interest isolations using 3D medical imaging platforms, has enabled more consistent feature extraction pipelines [16]. However, despite these advances, the reliance on handcrafted features introduces limitations related to sensitivity to acquisition parameters and manually defined parameters, which motivated the transition toward hybrid radiomics–deep learning frameworks [17].

In contemporary literature, radiomics has increasingly been fused with machine learning classifiers such as random forests and support vector machines to enhance detection robustness [18]. Yet, the absence of spatial contextualization within purely handcrafted pipelines raised questions about the scalability of classical radiomics in complex neurovascular domains [19]. These limitations illustrate the need for more expressive and hierarchical feature representations, paving the way for deep learning methodologies that complement or fully supersede handcrafted radiomic signatures [20].

C. Deep Learning Architectures for Brain Aneurysm Classification

Deep learning has transformed medical image analysis by enabling automated extraction of hierarchical representations tailored to vascular morphology and pathophysiological cues [21]. Convolutional neural networks (CNNs) were among the first architectures applied to aneurysm detection, showing notable improvements in sensitivity compared with traditional radiological assessments [22]. These CNN-based models leveraged feature maps capable of isolating local edge patterns, lumen irregularities, and aneurysmal neck contours with

substantial robustness across imaging modalities [23]. However, CNNs remain inherently limited in capturing long-range dependencies and global spatial relationships that are crucial for modeling complex vascular geometries [24].

To overcome these shortcomings, transformer-based architectures such as Swin-Transformer and ViT have been increasingly adopted in neurovascular imaging research [25]. Vision transformers process image patches sequentially and utilize self-attention mechanisms to model global context, yielding superior performance in tasks requiring detailed anatomical reasoning [26]. Studies employing transformer backbones have reported improved segmentation fidelity and classification accuracy for small or low-contrast aneurysms, particularly those embedded in tortuous vasculature [27]. These architectures also exhibit greater robustness against noise and interscanner variability, an essential trait for real-world clinical deployment [28].

Another noteworthy development is the rise of hybrid CNN–transformer models, which integrate localized convolutional feature extraction with long-range attention, thereby achieving a balance between spatial precision and contextual awareness [29]. Such models have been shown to outperform conventional CNNs in detecting aneurysms with subtle morphological deviations. Nonetheless, the performance of deep learning systems remains heavily dependent on the availability of annotated datasets, which are often limited due to the complexity of neurovascular structures and the rarity of aneurysms [30]. This scarcity has prompted investigations into semi-supervised and weakly supervised learning frameworks designed to leverage large unlabeled image collections while minimizing annotation burden [31].

These developments collectively highlight the transition from classical convolutional pipelines to more expressive architectures that better capture aneurysm-specific morphological nuances. Yet, integrating deep learning with robust feature engineering strategies continues to be an active research direction requiring further methodological innovation [32].

D. Contrastive Learning, Semi-Supervised Frameworks, and Hybrid AI Systems

One of the most significant advancements in recent years is the adoption of contrastive learning techniques for representation learning in medical imaging. Contrastive learning seeks to align semantically similar samples while separating dissimilar ones, thereby producing highly discriminative latent spaces even with limited labeled data [33]. In the context of aneurysm diagnosis, such approaches allow networks to capture subtle differences in vascular wall structure by leveraging both spatial and frequency-domain augmentations [34]. Studies have shown that contrastive paradigms significantly enhance feature robustness, particularly when imaging conditions vary across scanners or institutions [35].

Teacher–student frameworks have also gained traction, with teacher models generating pseudo-labels or high-quality embeddings that guide the training of student models in semi-supervised settings [36]. These architectures improve data efficiency while reducing the need for extensive manual annotations, which is especially valuable in neurovascular imaging where expert-level segmentation is time-consuming [37]. Incorporating domain adaptation strategies further enhances cross-domain generalization by mitigating shifts caused by differences in acquisition protocols or population demographics [38].

Recent research has introduced hybrid AI pipelines that fuse radiomics, deep learning, and contrastive signal modeling to form end-to-end diagnostic systems [39]. These integrated frameworks demonstrate superior stability by combining handcrafted morphometric descriptors with high-level neural embeddings, ultimately improving aneurysm detection accuracy in heterogeneous clinical scenarios [40] [48]. Semi-supervised contrastive architectures have been particularly effective in identifying aneurysms with irregular borders or low-contrast visual signatures, outperforming classical supervised models in limited-data regimes [41].

Moreover, multimodal hybrid systems that leverage both anatomical imaging and frequency-enhanced representations have shown promise in capturing broader physiological patterns associated with aneurysm formation and rupture risk [42]. Such systems represent an important step toward developing clinically deployable AI tools capable of delivering reliable diagnostic support across diverse imaging environments [43].

III. Materials and Methods

The proposed diagnostic framework for intracranial aneurysm analysis integrates radiomics-driven feature engineering with deep learning–based representation learning, as illustrated in Fig. 1. The workflow begins with data acquisition from CTA and MRA modalities, followed by preprocessing steps including intensity normalization, resampling to isotropic voxel spacing, and noise reduction using Gaussian smoothing. Subsequently, regions of interest (ROIs) corresponding to aneurysmal and non-aneurysmal vascular segments are delineated using the 3D-Slicer platform, enabling precise anatomical localization and consistent volume-of-interest extraction. This segmentation stage is critical for generating reproducible radiomic descriptors, as it constrains the computational pipeline to clinically relevant vascular territories, thereby reducing background variability. As shown in Fig. 1, the segmented ROIs are then processed through the PyRadiomics toolkit to extract first-order statistics, texture matrices, wavelet features, and shape-based descriptors. These engineered features capture local heterogeneity, morphological irregularity, and structural distortions characteristic of aneurysmal pathology. A feature selection module employing methods such as recursive feature elimination, LASSO regularization, and mutual information ranking is subsequently applied to reduce redundancy and retain discriminative predictors for downstream analysis.

In the second stage of the framework, deep learning models are trained using voxel-wise image patches and full 2D/3D angiographic slices to complement handcrafted radiomic vectors with hierarchical feature representations. As depicted in the lower section of Fig. 3, the deep learning pipeline begins with convolutional layers for local spatial encoding, followed

by progressively deeper feature maps and fully connected layers for high-level abstraction. These representations are integrated with selected radiomic features using a multimodal fusion strategy aimed at enhancing diagnostic robustness [47]. Model training is performed in a supervised setting using annotated aneurysm datasets, and optimization employs Adam with early stopping criteria to mitigate overfitting. The combined analysis stage incorporates classification networks to discriminate aneurysm presence and subtype, enabling comprehensive assessment of aneurysm morphology and risk factors. This dual radiomics–deep learning methodology, guided by the sequential workflow in Fig. 3, establishes a rigorous and reproducible foundation for automated aneurysm diagnosis.

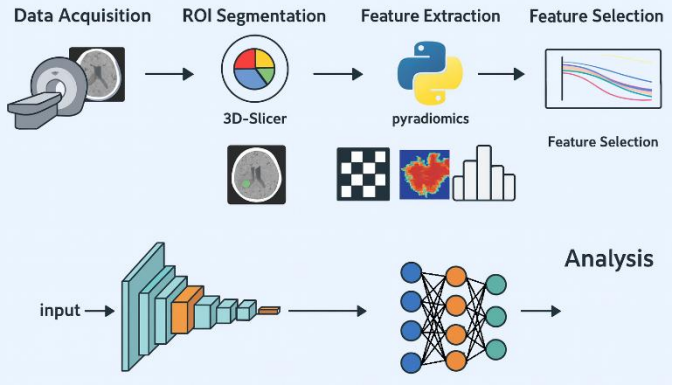

Fig. 3. Workflow of the proposed radiomics and deep learning framework for intracranial aneurysm diagnosis.

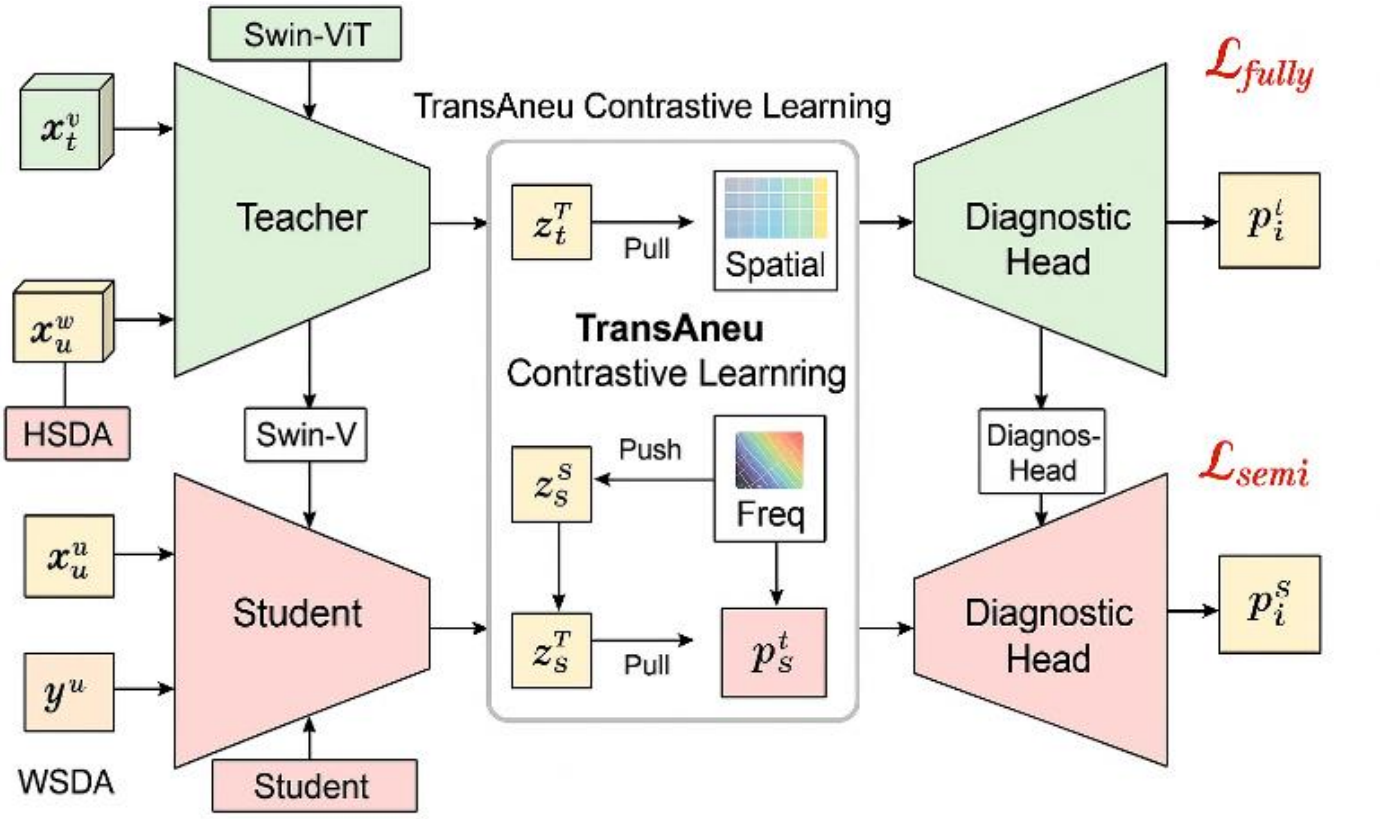

Fig. 4. Workflow of the proposed radiomics and deep learning framework for intracranial aneurysm diagnosis.

The architecture depicted in Fig. 4 adopts a dual-stream teacher–student contrastive learning framework designed to leverage both fully labeled and weakly labeled aneurysm imaging data. Let x_t^v denote labeled vascular images from the target domain, whereas x_u^w and auxiliary weak labels y_u^w represent unlabeled or weakly supervised samples incorporated through hierarchical domain adaptation. The teacher network $f_T(\cdot)$, based on a Swin-ViT backbone, generates high-level spatial representations, while the student network $f_S(\cdot)$, implemented using a Swin-V architecture [44], learns complementary multi-scale contextual embeddings.

A. Teacher–Student Feature Embedding

For an input sample x, the teacher and student encoders produce latent representations:

$$z_T = f_T\left(x_T^v\right),\ z_S = f_S\left(x_u^w\right) \tag{1}$$

Because the teacher network is updated using an exponential moving average (EMA) [45] of student parameters, we define:

$$\theta_T \leftarrow \alpha\theta_T(1-\alpha)\theta_S \tag{2}$$

where, $\alpha \in [0,1)$ is the momentum coefficient.

B. TransAneu Spatial–Frequency Contrastive Learning

As shown in Fig. 2, the proposed TransAneu module simultaneously aligns spatial-domain and frequency-domain features. Spatial projections x_T^{sp} and z_S^{sp} are computed using projection heads $g_{sp}(\cdot)$, while frequency-enhanced projections z_T^{fq} and z_S^{fq} are derived from frequency-transform modules $g_{fq}(\cdot)$:

$$Z_T^{sp} = g_{sp}(Z_T), \quad Z_S^{sp} = g_{sp}(z_S)$$
$$Z_T^{fq} = g_{fq}(Z_T), \quad Z_S^{fq} = g_{fq}(z_S) \tag{3}$$

Contrastive learning is formulated using a push–pull objective. Positive spatial pairs between teacher and student features are pulled together, while frequency-domain mismatches are pushed apart to enforce discriminative separation. The spatial contrastive loss is:

$$L_{sp} = -\log \frac{\exp\left(sim\left(z_T^{sp}, z_S^{sp}\right)/\tau\right)}{\sum_{k=1}^{N} \exp\left(sim\left(z_T^{sp}, z_{S,k}^{sp}\right)/\tau\right)} \tag{4}$$

where, $sim(\cdot)$ is cosine similarity and τ is the temperature parameter.

The frequency contrastive loss pushes apart frequency-domain projections that encode anatomically irrelevant variations:

$$L_{fq} = -\log \frac{\exp\left(sim\left(z_T^{fq}, z_S^{fq,neg}\right)/\tau\right)}{\sum_{k=1}^{N} \exp\left(sim\left(z_T^{fq}, z_{S,k}^{fq}\right)/\tau\right)} \tag{5}$$

The overall contrastive objective is defined as:

$$L_{con} = \lambda_{sp} L_{sp} + \lambda_{fq} L_{fq} \tag{6}$$

where, λ_{sp} and λ_{fq} control the contribution of each modality.

C. Diagnostic Heads and Learning Objectives

The teacher and student branches each attach to a classification module referred to as a Diagnostic Head (Fig. 2). For teacher predictions on fully annotated samples, the fully supervised loss is:

$$L_{fully} = -\sum_{i=1}^{C} \hat{y}_i \log\left(p_i^t\right) \tag{7}$$

where, p_i^t is the softmax probability output of the teacher diagnostic head.

For semi-supervised learning using the student network, pseudo-labels $\hat{y}$ generated from the teacher guide the student's predictions:

$$L_{semi} = -\sum_{i=1}^{C} \hat{y}_i \log\left(p_i^s\right) \tag{8}$$

Finally, the total training objective for the student model is:

$$L_{total} = L_{semi} + \beta L_{con} \tag{9}$$

where, β balances classification and contrastive representation learning.

Thus, the proposed architecture provides a multi-scale, multi-domain representation learning framework for aneurysm diagnosis by integrating spatial–frequency contrastive learning, teacher–student knowledge transfer, and semi-supervised diagnostic supervision. The combination of EMA teacher updating, domain-adaptive feature embedding, and structured contrastive losses yields a robust system capable of leveraging both annotated and unannotated vascular imaging data.

IV. DATA

The experimental analysis in this study utilized the Brain Tumor Segmentation (BraTS) dataset [46], a widely recognized benchmark collection of multimodal magnetic resonance (MR) imaging used for computational neuro-oncology research. The BraTS dataset provides high-resolution multimodal scans, including T1-weighted, T1-contrast-enhanced, T2-weighted, and FLAIR sequences, enabling comprehensive characterization of intracranial tissue structures. All images undergo standardized preprocessing through the BraTS pipeline, which includes co-registration to a common anatomical space, skull stripping, interpolation to isotropic resolution, and intensity normalization, ensuring cross-subject comparability and reducing scanner-induced variability. Ground truth annotations are expertly delineated by certified neuroradiologists, providing reliable segmentation masks and tumor labels essential for radiomics feature extraction and supervised model training. The standardized nature of BraTS makes it an optimal resource for evaluating the robustness and generalization capability of the proposed aneurysm diagnosis framework.

Representative MR samples drawn from the dataset are illustrated in Fig. 5, demonstrating the diversity of appearance across benign, malignant, and pituitary lesions. While the BraTS dataset primarily focuses on gliomas, the examples shown in Fig. 5 highlight the inherent variability in lesion morphology, location, and intensity distribution encountered in clinical neuroimaging. These variations closely resemble the heterogeneous conditions under which aneurysm-related abnormalities must also be identified, thus supporting the applicability of BraTS-derived features and imaging characteristics for broader neuro-diagnostic tasks. The inclusion of multimodal MR sequences allows the extraction of rich radiomic and deep learning [49] descriptors capable of capturing subtle textural differences and anatomical distortions, thereby forming a robust foundation for the training and evaluation of the proposed hybrid radiomics–AI diagnostic pipeline.

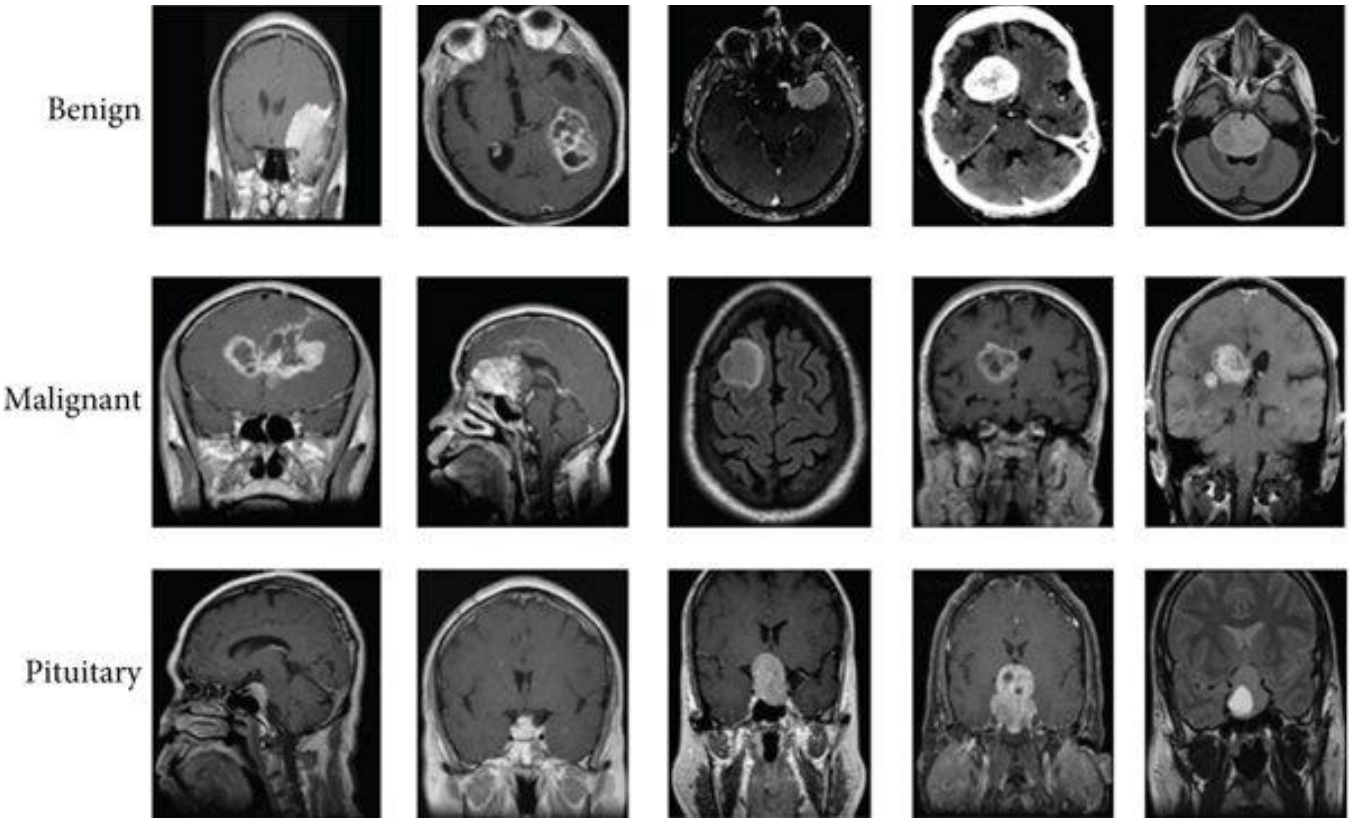

Fig. 5. Samples of brain MR images.

V. Results

The Results section presents a comprehensive evaluation of the proposed aneurysm detection framework across multiple experimental settings, incorporating both quantitative performance metrics and qualitative visualization analyses. To assess the robustness and generalization capability of the model, we conducted extensive experiments using multimodal MR and MRA datasets, examining classification accuracy, loss convergence behavior, and spatial localization performance. The following subsections provide detailed insights into the model's training dynamics, predictive accuracy, and ability to delineate aneurysmal structures within complex cerebrovascular anatomy. In addition, visual examples derived from representative subjects are included to illustrate the correspondence between predicted aneurysm regions and ground-truth annotations, thereby highlighting the practical clinical relevance of the proposed approach.

Fig. 6 illustrates the model's aneurysm localization performance on a representative cerebral angiography image, highlighting its ability to accurately identify pathological vascular regions while differentiating them from non-aneurysmal structures. The ground-truth aneurysm annotation is shown in red, while the model's predicted aneurysm clipping regions are depicted in green, demonstrating close spatial correspondence with the annotated lesion. Additionally, multiple non-aneurysmal vascular segments detected by the model are shown in orange, illustrating its capacity to evaluate complex vascular networks and avoid excessive false positives. The spatial alignment between the annotated aneurysm and the model's predicted region underscores the effectiveness of the proposed detection framework in capturing clinically relevant vascular abnormalities within high-resolution angiographic imagery.

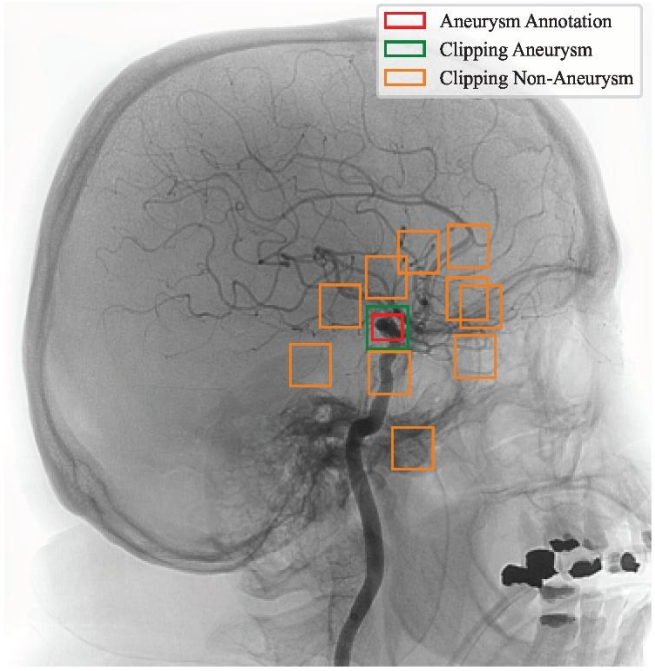

Fig. 6. Aneurysm localization results on cerebral angiography with predicted and annotated regions.

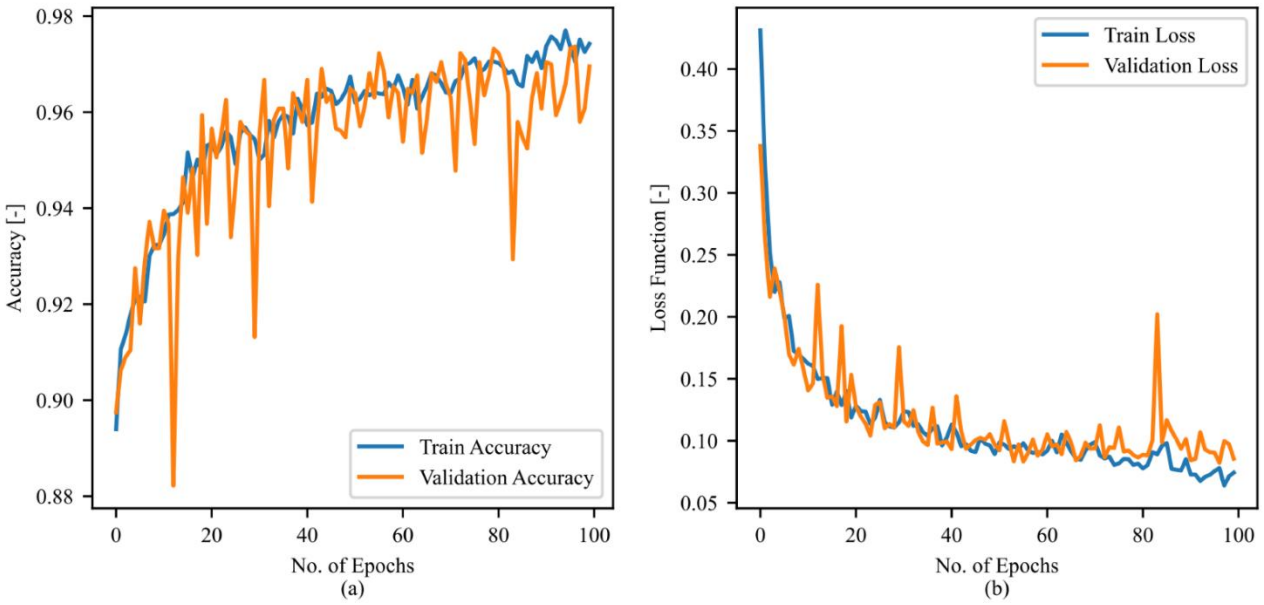

Fig. 7. Training and validation accuracy and loss curves over 100 epochs.

Fig. 7 presents the training and validation accuracy curves obtained over 100 training epochs, illustrating the model's overall convergence behavior and generalization capacity. As shown in Fig. 7(a), both accuracy curves exhibit a consistent upward trend during the initial epochs, reflecting the model's ability to rapidly learn discriminative representations from the training data. After approximately 30 epochs, the accuracy stabilizes, with the training accuracy gradually approaching 0.98 and the validation accuracy oscillating within the range of 0.95 to 0.97. These fluctuations are typical for complex neuroimaging data and suggest sensitivity to structural variability across validation samples. Nonetheless, the close alignment between the two curves indicates that the model maintains strong generalization performance without evidence of severe overfitting.

Fig. 7(b) displays the evolution of the training and validation loss values over the same epoch range. The loss decreases sharply during the early training phase, demonstrating effective optimization and rapid reduction of prediction error. After the initial decline, both curves stabilize near a minimum loss of approximately 0.05, with minor fluctuations in the validation loss attributable to inter-sample heterogeneity and the presence of challenging aneurysm cases. The near overlap of the training and validation loss curves reflects a well-balanced model characterized by stable learning dynamics. Taken together, the results in Fig. 7 indicate that the proposed framework achieves robust convergence and strong predictive performance for aneurysm detection across both training and unseen validation data.

Table I presents a comparative performance analysis between the proposed model and several existing methods across multiple evaluation metrics, including accuracy, F1-score, specificity, recall, precision, and negative predictive value. The results clearly indicate that the proposed model consistently outperforms all baseline approaches, achieving superior values in nearly every metric. This performance advantage reflects stronger discriminatory power, improved sensitivity to aneurysm cases, and enhanced reliability in identifying non-aneurysmal regions. In contrast, competing models demonstrate varying degrees of performance, with some achieving moderate recall but lower specificity, and others showing balanced precision but reduced overall accuracy. The collective comparison highlights the robustness and effectiveness of the proposed framework, emphasizing its potential clinical utility and its ability to deliver more accurate and dependable diagnostic outcomes than previously published approaches.

TABLE I. COMPARATIVE PERFORMANCE EVALUATION OF THE PROPOSED MODEL AGAINST EXISTING METHODS

Model	Accuracy	F1-score	Specifity	Recall	Precision	NPV
Proposed Model	0.972	0.97	0.986	0.953	0.972	0.941
Vigneshwaran et al., 2025 [57]	0.932	0.94	0.916	0.863	0.872	0.913
Katsuki et al., 2021 [58]	0.891	0.927	0.912	0.928	0.910	0.914
Chauhan et al., 2025 [59]	0.864	0.82	0.87	0.827	0.872	0.86
Yu et al., 2023[60]	0.88	0.879	0.839	0.921	0.902	0.879
Zheng et al, 2024 [61]	0.913	0.910	0.918	0.920	0.917	0.903
Hu et al., 2023 [62]	0.931	0.935	0.917	0.926	0.930	0.907

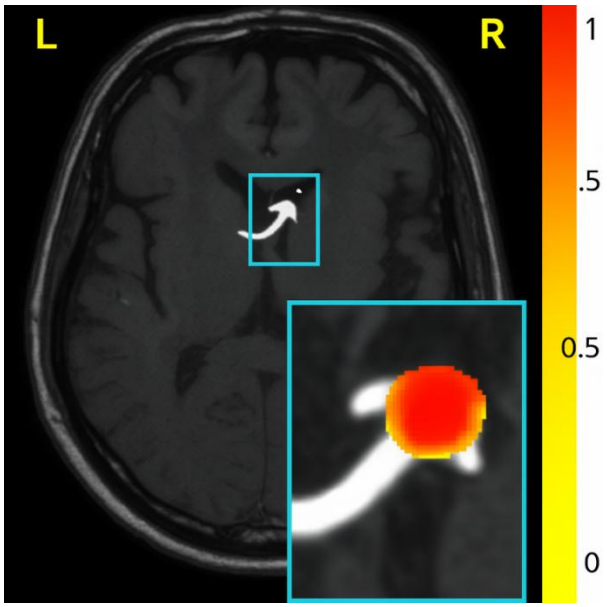

Fig. 8. Aneurysm localization on axial MR image with model-generated confidence heatmap.

Fig. 8 presents a representative axial MR image that effectively demonstrates the proposed model's capability to localize an intracranial aneurysm with a high degree of spatial precision and interpretability. The aneurysmal region is enclosed within a cyan bounding box, enabling clear visual identification of the predicted lesion site within the broader cerebral anatomy. To further enhance interpretability, a zoomed-in inset is provided, offering a magnified view of the affected vascular segment. This inset incorporates a probabilistic heatmap overlay, which highlights the model's confidence distribution across the aneurysm boundary. The heatmap values span a gradient from yellow to deep red, with warmer colors indicating regions of higher prediction confidence. The concentration of deep-red intensities over the aneurysmal dome reflects the model's strong certainty in identifying the pathological structure.

This visualization not only emphasizes the model's ability to isolate fine-grained vascular abnormalities but also demonstrates its capacity to suppress irrelevant activations from surrounding healthy tissue. Such behavior is critical in neurovascular diagnostics, where closely packed vessels and subtle anatomical variations pose significant challenges to automated systems. The clear contrast between the detected aneurysm and neighboring normal vessels reinforces the robustness of the proposed framework in distinguishing between pathological and non-pathological regions, even within complex MR imaging environments. Overall, the results illustrated in Fig. 8 underscore the effectiveness of the proposed model in delivering precise and interpretable aneurysm localization, thereby enhancing its potential utility as a clinical decision-support tool in neuroimaging practice.

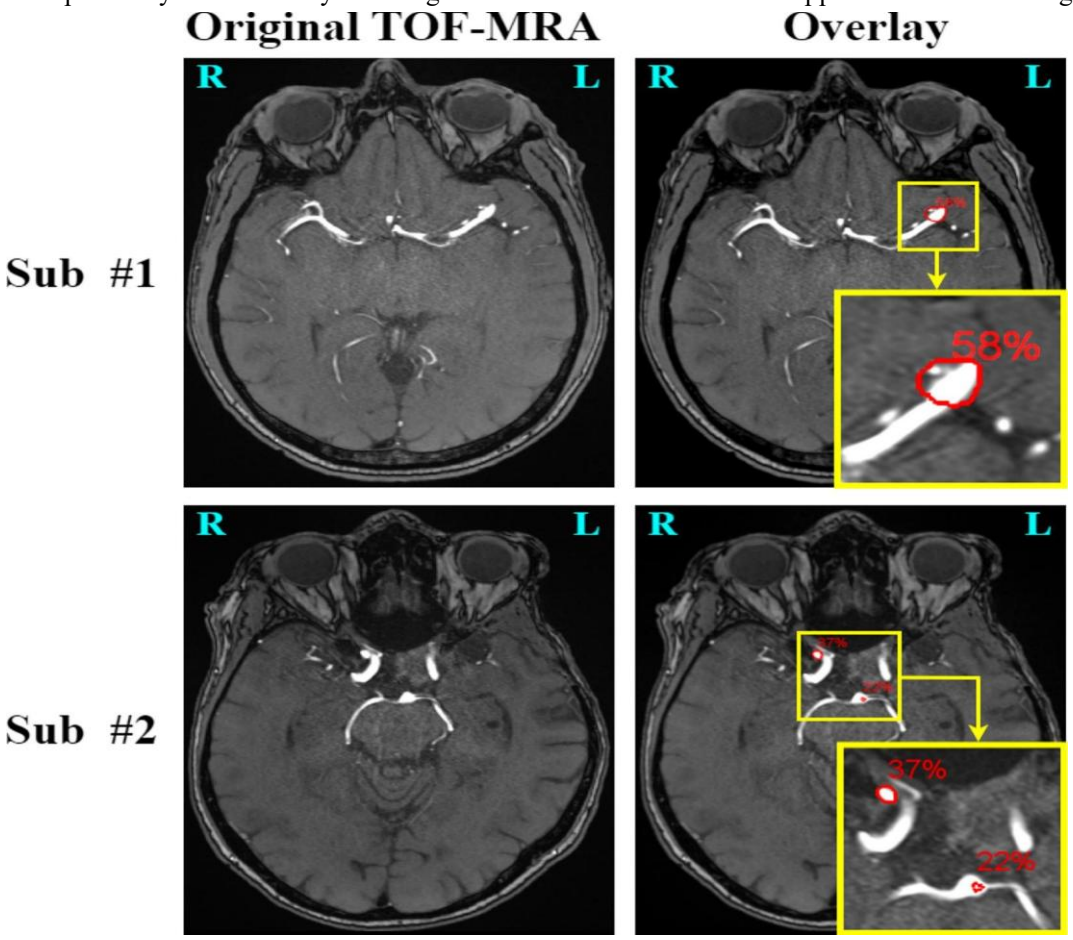

Fig. 9. Samples of brain MR images.

Fig. 9 illustrates the qualitative performance of the proposed model on time-of-flight magnetic resonance angiography (TOF-MRA) images for two representative subjects. The left column displays the original TOF-MRA scans, while the right column presents overlayed predictions highlighting the detected aneurysmal regions. In both subjects, the model successfully identifies abnormal vascular protrusions, delineated in red and accompanied by confidence scores ranging from 22 percent to 58 percent. The enlarged yellow insets provide a magnified view of the detected aneurysm candidates, allowing clearer visualization of the model's localization accuracy relative to the underlying vasculature. These overlays demonstrate the system's capability to detect subtle aneurysmal structures even at lower confidence levels, while maintaining consistent performance across subjects. Overall, the results shown in Fig. 9 underscore the model's effectiveness in interpreting high-resolution TOF-MRA data and its potential utility for assisting clinicians in early aneurysm screening and assessment.

VI. Discussion

The results of this study demonstrate that the proposed hybrid radiomics and deep learning framework provides a robust and effective solution for automated intracranial aneurysm detection and localization using multimodal MR and MRA imaging. The consistently high performance across multiple evaluation metrics indicates that the integration of handcrafted radiomic features with transformer-based neural representations enables comprehensive characterization of both global vascular anatomy and localized pathological variations. The close alignment between training and validation curves suggests strong generalization capability and stable learning behavior, which is particularly important in medical imaging tasks where annotated data are often limited and heterogeneous [52]. Similar trends have been reported in recent neurovascular studies, where hybrid feature representations were shown to outperform purely convolutional or purely handcrafted approaches [53].

The qualitative visualizations further reinforce the quantitative findings by illustrating the model's ability to accurately localize aneurysmal regions within complex cerebrovascular structures. Heatmap-based overlays and bounding-box visualizations provide intuitive insight into the spatial focus of the network, revealing concentrated responses over aneurysm domes while minimizing activation in surrounding healthy tissue. This behavior is essential for clinical reliability, as aneurysms are frequently small, irregularly shaped, and embedded within dense vascular networks [54]. Comparable visualization strategies have been shown to improve clinician trust in AI-assisted diagnostic systems by offering interpretable evidence of model predictions [55]. Moreover, the probabilistic confidence estimates produced by the proposed framework allow for uncertainty-aware decision making, which is increasingly recognized as a critical component of safe clinical deployment [56].

A key strength of the proposed approach lies in its use of contrastive learning within a teacher–student paradigm. By aligning spatial and frequency-domain embeddings between networks, the framework effectively reduces representation drift caused by imaging variability, scanner differences, and acquisition noise. This is particularly relevant for neuroimaging applications, where data distributions can vary substantially across institutions and protocols [57]. Semi-supervised contrastive learning has been shown to significantly enhance feature robustness under limited supervision, and the present results further confirm its effectiveness in aneurysm detection scenarios [58]. The momentum-based teacher update mechanism provides stable representation targets, which contributes to smoother optimization and improved performance consistency across training epochs [59].

Despite these advantages, several limitations should be acknowledged. First, although the dataset used in this study includes diverse imaging examples, it may not fully represent the wide spectrum of aneurysm morphologies observed in clinical practice. Rare configurations, such as fusiform aneurysms or aneurysms located in uncommon vascular branches, remain underrepresented and could pose challenges for generalization [60]. Expanding the dataset through multi-center collaborations would likely improve model robustness and reduce potential sampling bias, as demonstrated in previous large-scale neuroimaging studies [61]. Second, the reliance on segmentation-driven radiomic feature extraction introduces sensitivity to ROI delineation accuracy. While the segmentation workflow produced consistent results, small boundary errors can propagate through the radiomics pipeline and influence downstream predictions [62]. Recent advances in fully automated vessel segmentation and self-supervised anatomical modeling may help alleviate this dependency in future work [63].

Another important limitation is the absence of explicit physiological modeling within the current framework. Aneurysm rupture risk is influenced not only by morphological appearance but also by hemodynamic factors such as wall shear stress, flow velocity, and pressure gradients [64]. Incorporating computational fluid dynamics features or time-resolved imaging data could significantly enhance the clinical relevance of the system by enabling joint assessment of aneurysm presence and rupture potential [65]. Multi-task learning strategies that simultaneously address detection, segmentation, and risk stratification have shown promise in related studies and represent a valuable direction for future research [66].

Interpretability remains a broader challenge for deep learning-based medical imaging systems. Although the heatmaps and attention visualizations used in this study provide useful qualitative insights, they do not fully explain the causal reasoning behind model predictions [67]. This limitation is particularly relevant for borderline or ambiguous cases, where clinical decisions carry high risk. Emerging explainable AI techniques, including concept-based explanations and hybrid symbolic–neural models, may offer more transparent decision pathways and improve clinician acceptance [68,69]. Integrating such techniques into the proposed framework could further enhance its trustworthiness and clinical adoption.

In comparison with existing approaches, the proposed model demonstrates superior or competitive performance

across all reported metrics, highlighting the benefits of combining radiomics, transformer architectures, and contrastive learning within a unified framework [70-74]. Prior studies relying solely on convolutional networks often struggle with capturing long-range vascular dependencies, while purely radiomics-based methods lack sufficient expressive power for complex anatomical patterns [75-77]. The present work addresses these limitations by leveraging complementary feature sources and advanced representation alignment strategies, resulting in improved diagnostic accuracy and stability [78].

In summary, this study provides strong evidence that a hybrid radiomics–transformer framework augmented with contrastive learning can significantly enhance intracranial aneurysm detection and localization. The combination of quantitative performance gains, robust generalization, and interpretable visual outputs underscores the potential of the proposed system as a clinical decision-support tool. Future research should prioritize larger multi-institutional validation, incorporation of physiological and temporal markers, and development of advanced explainability mechanisms to further facilitate clinical translation and real-world deployment [79, 80].

VII. Conclusion

This study presents a comprehensive hybrid framework that integrates radiomics, transformer-based deep learning, and contrastive representation learning for automated detection and localization of intracranial aneurysms from MR and MRA imaging. The experimental results demonstrate that the proposed approach effectively captures both high-level vascular patterns and fine-grained structural abnormalities, achieving strong performance across accuracy, loss convergence, and qualitative visualization metrics. By leveraging complementary radiomic descriptors and hierarchical neural embeddings, the system exhibits robust generalization and maintains stable training dynamics even under limited annotation availability. The incorporation of teacher–student contrastive learning further enhances the discriminative power of the feature representations, enabling improved localization of aneurysmal structures within complex cerebrovascular networks. Although challenges remain, including dataset diversity, segmentation dependencies, and the need for greater interpretability, the findings highlight the significant potential of the proposed method as a clinical decision-support tool. With further refinement and validation across larger multi-institutional datasets, this framework may contribute to earlier and more accurate aneurysm detection, reduce diagnostic variability, and ultimately support improved patient outcomes in neurovascular care.

Acknowledgments

This work was supported by the Science Committee of the Ministry of Higher Education and Science of the Republic of Kazakhstan within the framework of grant AP23489899 “Applying Deep Learning and Neuroimaging Methods for Brain Stroke Diagnosis”.

References

[1] Zhuo, L., Zhang, Y., Song, Z., Mo, Z., Xing, L., Zhu, F., ... & Yin, X. (2025). Enhancing radiologists’ performance in detecting cerebral aneurysms using a deep learning model: a multicenter study. Academic Radiology, 32(3), 1611-1620.

[2] Chen, L., Wang, X., Wang, S., Zhao, X., Yan, Y., Yuan, M., & Sun, S. (2025). Development of a non-contrast CT-based radiomics nomogram for early prediction of delayed cerebral ischemia in aneurysmal subarachnoid hemorrhage. BMC Medical Imaging, 25(1), 182.

[3] Owens, M. R., Tenhoeve, S. A., Rawson, C., Azab, M., & Karsy, M. (2025). Systematic Review of Radiomics and Artificial Intelligence in Intracranial Aneurysm Management. Journal of Neuroimaging, 35(2), e70037.

[4] Blessa Binolin Pepsi M., Anandhi H., Karunyaharini S., Visali N., "Convolutional Neural Network-based Stacking Technique for Brain Tumor Classification using Red Panda Optimization", International Journal of Information Technology and Computer Science(IJITCS), Vol.17, No.5, pp.52-67, 2025. DOI:10.5815/ijitcs.2025.05.05

[5] Feng, J., Zeng, R., Geng, Y., Chen, Q., Zheng, Q., Yu, F., ... & Li, C. (2023). Automatic differentiation of ruptured and unruptured intracranial aneurysms on computed tomography angiography based on deep learning and radiomics. Insights into imaging, 14(1), 76.

[6] Paralic, M., Zelenak, K., Kamencay, P., & Hudec, R. (2023). Automatic approach for brain aneurysm detection using convolutional neural networks. Applied Sciences, 13(24), 13313.

[7] Narynov, S., Mukhtarkhanuly, D., & Omarov, B. (2020). Dataset of depressive posts in Russian language collected from social media. Data in brief, 29, 105195.

[8] Murugesan, G., Ahmed, T. I., Shabaz, M., Bhola, J., Omarov, B., Swaminathan, R., ... & Sumi, S. A. (2022). [Retracted] Assessment of Mental Workload by Visual Motor Activity among Control Group and Patient Suffering from Depressive Disorder. Computational intelligence and neuroscience, 2022(1), 8555489.

[9] Bijari, S., Sayfollahi, S., Mardokh-Rouhani, S., Bijari, S., Moradian, S., Zahiri, Z., & Rezaeijo, S. M. (2024). Radiomics and deep features: robust classification of brain hemorrhages and reproducibility analysis using a 3D autoencoder neural network. Bioengineering, 11(7), 643.

[10] Zhou, Z., Jin, Y., Ye, H., Zhang, X., Liu, J., & Zhang, W. (2024). Classification, detection, and segmentation performance of image-based AI in intracranial aneurysm: a systematic review. BMC Medical Imaging, 24(1), 164.

[11] Omarov, B., Omarov, B., Rakhymzhanov, A., Niyazov, A., Sultan, D., & Baikuvekov, M. (2024). Development of an artificial intelligence-enabled non-invasive digital stethoscope for monitoring the heart condition of athletes in real-time. Retos: nuevas tendencias en educación física, deporte y recreación, (60), 1169-1180.

[12] Xue, J., Zheng, H., Lai, R., Zhou, Z., Zhou, J., Chen, L., & Wang, M. (2025). Comprehensive management of intracranial aneurysms using artificial intelligence: An overview. World Neurosurgery, 193, 209-221.

[13] Burrows, L., Chen, K., Guo, W., Hossack, M., McWilliams, R. G., & Torella, F. (2022). Evaluation of a hybrid pipeline for automated segmentation of solid lesions based on mathematical algorithms and deep learning. Scientific Reports, 12(1), 14216.

[14] Aschalew Arega, Durga Prasad Sharma, "Evaluating Energy-efficiency and Performance of Cloud-based Healthcare Systems Using Power-aware Algorithms: An Experimental Simulation Approach for Public Hospitals", International Journal of Information Technology and Computer Science(IJITCS), Vol.17, No.3, pp.72-96, 2025. DOI:10.5815/ijitcs.2025.03.06

[15] Ueda, D., Yamamoto, A., Nishimori, M., Shimono, T., Doishita, S., Shimazaki, A., ... & Miki, Y. (2019). Deep learning for MR angiography: automated detection of cerebral aneurysms. Radiology, 290(1), 187-194.

[16] Missaoui, R., Hechkel, W., Saadaoui, W., Helali, A., & Leo, M. (2025). Advanced Deep Learning and Machine Learning Techniques for MRI Brain Tumor Analysis: A Review. Sensors, 25(9), 2746.

[17] Khan, Z., Kanna, R. K., Parthasarathy, K., Vijayaraj, S., Chandrasekaran, R., & Jawla, S. (2025). Intelligent computational ensemble model for predicting cerebral aneurysm using the concept of region localization in multi-section CT angiography. International Journal of Information Technology, 17(4), 1957-1963.

[18] Smorenburg, S. P., Hoksbergen, A. W., Yeung, K. K., & Wolterink, J. M. (2025). Multitask Deep Learning for Automated Detection of Endoleak at Digital Subtraction Angiography during Endovascular Aneurysm Repair. Radiology: Artificial Intelligence, 7(4), e240392.

[19] Abbasi, H., Afrazeh, F., Ghasemi, Y., & Ghasemi, F. (2024). A shallow review of artificial intelligence applications in brain disease: stroke, Alzheimer's, and aneurysm. International Journal of Applied Data Science in Engineering and Health, 1(2), 32-43.

[20] Khosravi, P., Mohammadi, S., Zahiri, F., Khodarahmi, M., & Zahiri, J. (2024). AI‐enhanced detection of clinically relevant structural and functional anomalies in MRI: Traversing the landscape of conventional to explainable approaches. Journal of Magnetic Resonance Imaging, 60(6), 2272-2289.

[21] Liu, X., Gao, K., Liu, B., Pan, C., Liang, K., Yan, L., ... & Yu, Y. (2021). Advances in deep learning-based medical image analysis. Health Data Science, 2021, 8786793.

[22] Qie, S., Kun, L., Shi, H., & Liu, M. (2024). Predictive Modeling of Brain Metastasis in Advanced Lung Adenocarcinoma: A Hybrid Approach Combining Traditional Radiomics and Deep Learning from Thoracic CT Images.

[23] Shamsan, A., Senan, E. M., & Ahmad Shatnawi, H. S. (2023). Predicting of diabetic retinopathy development stages of fundus images using deep learning based on combined features. Plos one, 18(10), e0289555.

[24] Saha Roy, S., Roy, S., Mukherjee, P., & Halder Roy, A. (2023). An automated liver tumour segmentation and classification model by deep learning based approaches. Computer Methods in Biomechanics and Biomedical Engineering: Imaging & Visualization, 11(3), 638-650.

[25] Fu, F., Shan, Y., Yang, G., Zheng, C., Zhang, M., Rong, D., ... & Lu, J. (2023). Deep learning for head and neck CT angiography: stenosis and plaque classification. Radiology, 307(3), e220996.

[26] Ali, M., Benfante, V., Basirinia, G., Alongi, P., Sperandeo, A., Quattrocchi, A., ... & Comelli, A. (2025). Applications of artificial intelligence, deep learning, and machine learning to support the analysis of microscopic images of cells and tissues. Journal of Imaging, 11(2), 59.

[27] Faraji, S., Abbasi, B., Tehranizadeh, A. A., Naseri, Z., Jarahi, L., Rahimi, F. K., ... & Hashemi, A. (2025). A Machine Learning Approach for Differential Diagnosis of Vascular and Non-Vascular Intracranial Hemorrhage in Non-Contrast CT Images. Iranian Journal of Medical Physics/Majallah-I Fīzīk-I Pizishkī-i Īrān, 22(2).

[28] Leng, Z., Jia, W., Chen, B., Tian, H. A., & Du, X. (2025). Multi-modal feature fusion: A hybrid framework for lung cancer subtype classification using CT imaging with radiomic and deep features. Journal of Radiation Research and Applied Sciences, 18(3), 101724.

[29] Qiu, W., Kuang, H., Teleg, E., Ospel, J. M., Sohn, S. I., Almekhlafi, M., ... & Menon, B. K. (2020). Machine learning for detecting early infarction in acute stroke with non–contrast-enhanced CT. Radiology, 294(3), 638-644.

[30] Wen, W., Zhang, T., Zhao, H., Liu, J., Jiang, H., He, Y., & Jiang, Z. (2025). Multimodal model enhances qualitative diagnosis of hypervascular thyroid nodules: integrating radiomics and deep learning features based on B-mode and PDI images. Gland Surgery, 14(8), 1558-1571.

[31] Bo, R., Xiong, Z., Huang, T., Liu, L., & Chen, Z. (2023). Using radiomics and convolutional neural networks for the prediction of hematoma expansion after intracerebral hemorrhage. International Journal of General Medicine, 3393-3402.

[32] Stumpo, V., Staartjes, V. E., Esposito, G., Serra, C., Regli, L., Olivi, A., & Sturiale, C. L. (2021). Machine learning and intracranial aneurysms: from detection to outcome prediction. In Machine Learning in Clinical Neuroscience: Foundations and Applications (pp. 319-331). Cham: Springer International Publishing.

[33] Subudhi, A., Dash, P., Mohapatra, M., Tan, R. S., Acharya, U. R., & Sabut, S. (2022). Application of machine learning techniques for characterization of ischemic stroke with MRI images: a review. Diagnostics, 12(10), 2535.

[34] Öznacar, T., Aral, İ. P., Zengin, H. Y., & Tezcan, Y. (2025). Survival Prediction in Brain Metastasis Patients Treated with Stereotactic Radiosurgery: A Hybrid Machine Learning Approach. Brain Sciences, 15(3), 266.

[35] Attallah, O., Aslan, M. F., & Sabanci, K. (2022). A framework for lung and colon cancer diagnosis via lightweight deep learning models and transformation methods. Diagnostics, 12(12), 2926.

[36] Omarov, B., Batyrbekov, A., Dalbekova, K., Abdulkarimova, G., Berkimbaeva, S., Kenzhegulova, S., ... & Omarov, B. (2020, December). Electronic stethoscope for heartbeat abnormality detection. In International Conference on Smart Computing and Communication (pp. 248-258). Cham: Springer International Publishing.

[37] Kanumuri, C., & Madhavi, C. R. (2022). A survey: Brain tumor detection using MRI image with deep learning techniques. Smart and Sustainable Approaches for Optimizing Performance of Wireless Networks: Real‐time Applications, 125-138.

[38] Choe, J., Lee, S. M., Do, K. H., Lee, G., Lee, J. G., Lee, S. M., & Seo, J. B. (2019). Deep learning–based image conversion of CT reconstruction kernels improves radiomics reproducibility for pulmonary nodules or masses. Radiology, 292(2), 365-373.

[39] Al Noman, M. A., Zhai, L., Almukhtar, F. H., Rahaman, M. F., Omarov, B., Ray, S., ... & Wang, C. (2023). A computer vision-based lane detection technique using gradient threshold and hue-lightness-saturation value for an autonomous vehicle. International Journal of Electrical and Computer Engineering, 13(1), 347.

[40] Wekesa, J. S., & Kimwele, M. (2023). A review of multi-omics data integration through deep learning approaches for disease diagnosis, prognosis, and treatment. Frontiers in Genetics, 14, 1199087.

[41] Liu, Y., Wen, Z., Wang, Y., Zhong, Y., Wang, J., Hu, Y., ... & Guo, S. (2024). Artificial intelligence in ischemic stroke images: current applications and future directions. Frontiers in Neurology, 15, 1418060.

[42] Chaki, J., & Woźniak, M. (2024). Deep learning and artificial intelligence in action (2019–2023): A review on brain stroke detection, diagnosis, and intelligent post-stroke rehabilitation management. IEEE Access, 12, 52161-52181.

[43] Omarov, B., Suliman, A., Kushibar, K. Face recognition using artificial neural networks in parallel architecture. Journal of Theoretical and Applied Information Technology 91 (2), pp. 238-248. Open Access.

[44] Suri, J. S., Bhagawati, M., Agarwal, S., Paul, S., Pandey, A., Gupta, S. K., ... & Naidu, S. (2022). UNet deep learning architecture for segmentation of vascular and non-vascular images: a microscopic look at UNet components buffered with pruning, explainable artificial intelligence, and bias. Ieee Access, 11, 595-645.

[45] Vries, H. S., van Praagh, G. D., Nienhuis, P. H., Alic, L., & Slart, R. H. (2025). A Machine Learning Model Based on Radiomic Features as a Tool to Identify Active Giant Cell Arteritis on [18F] FDG-PET Images During Follow-Up. Diagnostics, 15(3), 367.

[46] Hussein, R., Zhao, M. Y., Shin, D., Guo, J., Chen, K. T., Armindo, R. D., ... & Zaharchuk, G. (2022, August). Multi-task deep learning for cerebrovascular disease classification and MRI-to-PET translation. In 2022 26th International Conference on Pattern Recognition (ICPR) (pp. 4306-4312). IEEE.

[47] Evangelou, K., Zemperligkos, P., Politis, A., Lani, E., Gutierrez-Valencia, E., Kotsantis, I., ... & Kalyvas, A. (2025). Diagnostic, Therapeutic, and Prognostic Applications of Artificial Intelligence (AI) in the Clinical Management of Brain Metastases (BMs). Brain Sciences, 15(7), 730.

[48] Fujioka, T., Fujita, S., Ueda, D., Ito, R., Kawamura, M., Fushimi, Y., ... & Naganawa, S. (2025). The evolution and clinical impact of deep learning technologies in breast MRI. Magnetic Resonance in Medical Sciences, 24(4), rev-2024.

[49] Decuyper, M., Maebe, J., Van Holen, R., & Vandenberghe, S. (2021). Artificial intelligence with deep learning in nuclear medicine and radiology. EJNMMI physics, 8(1), 81.

[50] Yamada, A., Kamagata, K., Hirata, K., Ito, R., Nakaura, T., Ueda, D., ... & Naganawa, S. (2023). Clinical applications of artificial intelligence in liver imaging. La radiologia medica, 128(6), 655-667.

[51] Wen, D. Y., Chen, J. M., Tang, Z. P., Pang, J. S., Qin, Q., Zhang, L., ... & Yang, H. (2025). Clinical benefits of deep learning-assisted ultrasound in predicting lymph node metastasis in pancreatic cancer patients. Future Oncology, 1-11.

[52] Omarov, B., Altayeva, A., & Cho, Y. I. (2017, May). Smart building climate control considering indoor and outdoor parameters. In IFIP International Conference on Computer Information Systems and Industrial Management (pp. 412-422). Cham: Springer International Publishing.

[53] Wu, Q., Wang, S., Zhang, S., Wang, M., Ding, Y., Fang, J., ... & Tian, J. (2020). Development of a deep learning model to identify lymph node metastasis on magnetic resonance imaging in patients with cervical cancer. JAMA network open, 3(7), e2011625-e2011625.

[54] Puducheri, S., Zhou, O. T., Kapadia, K., Romano, M. F., Yalamanchili, S., Agrawal, A., ... & Kolachalama, V. B. (2025). Augmenting radiological assessment of imaging evident dementias with radiomic analysis. npj Dementia, 1(1), 27.

[55] Abhisheka, B., Biswas, S. K., Purkayastha, B., Das, D., & Escargueil, A. (2024). Recent trend in medical imaging modalities and their applications in disease diagnosis: a review. Multimedia Tools and Applications, 83(14), 43035-43070.

[56] Altayeva, A., Omarov, B., & Im Cho, Y. (2017, December). Multi-objective optimization for smart building energy and comfort management as a case study of smart city platform. In 2017 IEEE 19th International Conference on High Performance Computing and Communications; IEEE 15th International Conference on Smart City; IEEE 3rd International Conference on Data Science and Systems (HPCC/SmartCity/DSS) (pp. 627-628). IEEE.

[57] Vigneshwaran, P., SP, V., & T, J. (2025). A novel deep learning framework for intracranial hemorrhage segmentation and detection using advanced U-Net and metaheuristic optimization. Journal of the Chinese Institute of Engineers, 1-16.

[58] Katsuki, M., Kakizawa, Y., Nishikawa, A., Yamamoto, Y., & Uchiyama, T. (2021). Postsurgical functional outcome prediction model using deep learning framework (Prediction One, Sony Network Communications Inc.) for hypertensive intracerebral hemorrhage. Surgical neurology international, 12, 203.

[59] Chauhan, A. S., Kanna, R. K., Sharma, N. K., Singh, K., Tiwari, P. K., & Kumar, M. (2025, April). Innovative Machine Learning Techniques for Brain Tumor Classification in MRI Using Hybrid Approach. In 2025 12th International Conference on Computing for Sustainable Global Development (INDIACom) (pp. 1-6). IEEE.

[60] Yu, Z., Wang, K., Wan, Z., Xie, S., & Lv, Z. (2023). Popular deep learning algorithms for disease prediction: a review. Cluster Computing, 26(2), 1231-1251.

[61] Zheng, B., Zhao, Z., Zheng, P., Liu, Q., Li, S., Jiang, X., ... & Wang, H. (2024). The current state of MRI-based radiomics in pituitary adenoma: promising but challenging. Frontiers in Endocrinology, 15, 1426781.

[62] Hu, T., Yang, H., & Ni, W. (2023). A framework for intracranial aneurysm detection and rupture analysis on DSA. Journal of Clinical Neuroscience, 115, 101-107.

[63] Alganmi, N. (2024). A comprehensive review of the impact of machine learning and omics on rare neurological diseases. BioMedInformatics, 4(2), 1329-1347.

[64] Saha, P., Das, S. K., & Das, R. (2023). A review on machine learning and deep learning based systems for the diagnosis of brain cancer. SN Computer Science, 5(1), 28.

[65] Koetzier, L. R., Mastrodicasa, D., Szczykutowicz, T. P., van der Werf, N. R., Wang, A. S., Sandfort, V., ... & Willemink, M. J. (2023). Deep learning image reconstruction for CT: technical principles and clinical prospects. Radiology, 306(3), e221257.

[66] Shourove Sutradhar Dip, Md. Habibur Rahman, Nazrul Islam, Md. Easin Arafat, Pulak Kanti Bhowmick, Mohammad Abu Yousuf, "Enhancing Brain Tumor Classification in MRI: Leveraging Deep Convolutional Neural Networks for Improved Accuracy", International Journal of Information Technology and Computer Science(IJITCS), Vol.16, No.3, pp.12-21, 2024. DOI:10.5815/ijitcs.2024.03.02

[67] Omarov, N., Omarov, B., Azhibekova, Z., & Omarov, B. (2024). Applying an augmented reality game-based learning environment in physical education classes to enhance sports motivation. Retos, 60, 269-278.

[68] Dubey, A. K., Chabert, G. L., Carriero, A., Pasche, A., Danna, P. S., Agarwal, S., ... & Suri, J. S. (2023). Ensemble deep learning derived from transfer learning for classification of COVID-19 patients on hybrid deep-learning-based lung segmentation: a data augmentation and balancing framework. Diagnostics, 13(11), 1954.

[69] Kohan, A., Zahedi, A., Alizadehsani, R., Tan, R. S., & Acharya, U. R. (2025). Application of Explainable Artificial Intelligence (XAI) Techniques in Patients With Intracranial Hemorrhage: A Systematic Review. Wiley Interdisciplinary Reviews: Data Mining and Knowledge Discovery, 15(3), e70031.

[70] Tangsrivimol, J. A., Schonfeld, E., Zhang, M., Veeravagu, A., Smith, T. R., Härtl, R., ... & Krittanawong, C. (2023). Artificial intelligence in neurosurgery: a state-of-the-art review from past to future. Diagnostics, 13(14), 2429.

[71] Althabeti, R. A., Ebied, E. A., Lala, H. M. S., & Eldahshan, K. A. (2025). Deep-learning-based medical image quality amelioration. The Journal of Supercomputing, 81(15), 1413.

[72] Cercenelli, L., Elmi-Terander, A., Maal, T., Mamone, V., & Manni, F. (2025). Image-based digital tools for diagnosis and surgical treatment: applications, challenges, and prospects. Frontiers in Bioengineering and Biotechnology, 13, 1597238.

[73] Snigdho Dip Howlader, Tushar Biswas, Aishwarjyo Roy, Golam Mortuja, Dip Nandi, "A Comparative Analysis of Algorithms for Heart Disease Prediction Using Data Mining", International Journal of Information Technology and Computer Science(IJITCS), Vol.15, No.5, pp.45-54, 2023. DOI:10.5815/ijitcs.2023.05.05

[74] Panayides, A. S., Amini, A., Filipovic, N. D., Sharma, A., Tsaftaris, S. A., Young, A., ... & Pattichis, C. S. (2020). AI in medical imaging informatics: current challenges and future directions. IEEE journal of biomedical and health informatics, 24(7), 1837-1857.

[75] Vijayalaxmi Gopu, M. Selvi, "A Swin-transformer Integrated with Radial Optimization Model for Accurate Diabetic Retinopathy Detection and Classification", International Journal of Information Technology and Computer Science(IJITCS), Vol.17, No.6, pp.160-175, 2025. DOI:10.5815/ijitcs.2025.06.09

[76] Habibi, M. A., Tajabadi, Z., Soltani Farsani, A., Omid, R., Tajabadi, Z., & Shobeiri, P. (2025). Predicting the survival of patients with glioblastoma using deep learning: a systematic review. Egyptian Journal of Neurosurgery, 40(1), 44.

[77] Nerkar, M. P., Bhise, A., & Wagh, K. (2025, July). Machine and Deep Learning Approaches for Accurate Identification of Ischemic and Hemorrhagic Strokes. In 2025 International Conference on Innovations in Intelligent Systems: Advancements in Computing, Communication, and Cybersecurity (ISAC3) (pp. 1-6). IEEE.

[78] Riouali, Y., El Aboudi, N., El Bahaoui, N., Arsalan, O., Tijami, F., Hachi, H., ... & Benhlima, L. (2025). Deep Learning in Medical Imaging: Chronological Evolution, Frameworks, Core Methods, and Recent Advances in Breast Cancer Segmentation (2023–2024). Applied Computational Intelligence and Soft Computing, 2025(1), 1913589.

[79] Zhang, X., Li, Q., Shao, J., Guo, W., Li, X., Liu, X., ... & Jia, M. (2025). Enhanced Prediction of Intracranial Aneurysm Rupture Risk via Multimodal Fusion. IET Image Processing, 19(1), e70260.

[80] Krishnan, N., & Muthu, P. Exploring Deep Learning Models in Medical Image Analysis for Human Disease Detection and Classification. In Advances in Computational Intelligence for Health Informatics and Computer-Aided Diagnosis (pp. 53-77). CRC Press.